Brain Organization Underlying Superior Mathematical Abilities in Children with Autism

Supplemental Information

Supplemental Methods

Monte Carlo Procedures Used to Correct for Family-Wise Error Rate

We used a non-parametric approach based on Monte Carlo simulations to determine the minimum cluster size that controls for false positive rate at $p < 0.001$ for height and $p < .01$ for cluster extent. Monte Carlo simulations were implemented in MATLAB using methods similar to the AlphaSim procedure in the software package Analysis of Functional NeuroImages (AFNI) (1, 2). Ten thousand iterations of random 3D images, with the same resolution and dimensions as the fMRI data, were generated. The resulting images were masked for gray matter and then smoothed with the same 6 mm full-width half-maximum Gaussian kernel used to smooth the fMRI data. The maximum cluster size was then computed for each iteration and the probability distribution was estimated across the 10,000 iterations. The cluster threshold corresponding to a family-wise error significance level of height $p < .001$ and cluster extent $p < 0.01$ was determined to be 41 and 45 voxels for the univariate and multivariate analyses, respectively.

Multivariate Analysis

The multivariate pattern analysis (MVPA) analysis used a nonlinear classifier based on support-vector machine algorithms with radial basis function (RBF) kernels (3). At each voxel v_i, a 3 x 3 x 3 neighborhood (searchlight) centered at v_i was defined. Therefore, the spatial pattern of voxels in this neighborhood was defined by a 27-dimentional vector. Support vector machine

(SVM) classification was performed using LIBSVM (http://www.csie.ntu.edu.tw/~cjlin/libsvm) software. For the non-linear SVM classifier, we specified two parameters: C (regularization) and α (parameter RBF kernel) at each searchlight position. Subsequently we estimated optimal values of C, α as well as the generalizability of the classifier at each searchlight position by using a combination of grid cell and cross-validation procedures. Contrary to previous approaches in which the free parameter C was arbitrarily set (4), we here optimize both free parameters (C and α) based on the data, thereby designing an optimal classifier. At each voxel, a Leave-One-Out Cross Validation (LOOCV) procedure (5, 6) was used to measure the performance of the classifier in distinguishing children with autism spectrum disorder (ASD) from typically developing (TD) children during arithmetical problem solving. One single observation was used for testing the optimal classifier that was trained using the remaining observations. This process was repeated such that every observation was used once for testing purposes. For each iteration, the class label estimated by the optimal classifier was compared against the class label of the test observation. The ratio of correctly estimated class labels to the total number of observations, hereafter referred to as cross-validation accuracy (CVA), was then computed. The resulting 3D map of CVA at every voxel was used to identify brain regions that distinguish between the groups. Under the null hypothesis that there is no difference between the two groups, the CVAs were assumed to follow the binomial distribution B (N, p) with parameters N equal to the total number of participants in the two groups and *p* equal to 0.5, assuming that under the null hypothesis, the probability of each group is equal. The CVAs were then converted to *p*-values using the binomial distribution (5, 7).

Support Vector Regression Analysis

We used support vector regression (SVR) with the default settings of C = 1 and nu = 0.05, as implemented in the LIBSVM Toolbox (http://www.csie.ntu.edu.tw/~cjlin/libsvm/). We first estimated R^2, using the LOOCV procedure (see above). Each sample was designated the test sample in turns while the remaining samples were used to train the SVR predictor. The decision function derived from the training sample was then used to make a real-valued prediction about the test sample. R^2 was computed based on the observed and predicted values. Finally, the statistical significance of the SVR model was assessed using non-parametric analysis. The empirical null distribution of R^2 was estimated by generating 10,000 surrogate datasets under the null hypothesis that there was no association between *Numerical Operations* scores and functional activation patterns. Each surrogate dataset D_i of size equal to the observed dataset was generated by permuting the labels (*Numerical Operations* scores) on the observed data points. The SVR model was fitted to predict labels of each surrogate dataset D_i . R_i^2 was computed using the actual labels of D_i and predicted labels. This procedure produces a null distribution of R^2 of the SVR model. The statistical significance (p value) of the model was then determined by counting the number of R_i^2 greater than R^2 and dividing that count by the number of D_i (10,000).

Supplemental Results

Univariate Analyses

Between-group analysis using Rest as control. Between-group *t*-tests on the Simple addition problems versus Rest comparison did not reveal significant differences between children with ASD and their TD peers (height threshold: $p < .001$, extent threshold: $p < .01$).

Similarly, no differences were observed for the Complex addition problems versus Rest between-group comparison (height threshold: $p < .001$, extent threshold: $p < .01$).

Multivariate Analyses

Between-group analysis using Rest as the control condition. The main goal of multivariate analyses was to examine arithmetic-complexity related differences in brain activity patterns between ASD and TD children (**Figure 2**). Additional analyses were conducted to examine whether the observed multivariate activation pattern differences arose from group differences in the Simple addition problems. To address this question, group differences in multivariate activation patterns were examined for Simple addition problems contrasted with Rest. Virtually no overlap was observed with findings from our original arithmetic complexity related analysis (**Figure S1A**). Next we examined group differences in multivariate activation patterns for Complex addition problems contrasted with the Rest baseline. In this case, significant overlapping effects were observed in the ventral temporal-occipital cortex (VTOC) encompassing the fusiform gyrus (FG) and the inferior lateral occipital cortex (LOC), and in posterior parietal cortex encompassing the angular gyrus (AG) (**Figure S1B**). No overlapping effects were evident in the medial temporal lobe, a region in which the Rest baseline is known to vary significantly across individuals (8). Taken together, these analyses indicate that our arithmetic-complexity related findings are not driven by differences in brain activation patterns to Simple addition problems. These results also indicate that group differences in multivariate activation patterns are not additive, and that MVPA requires careful attention to experimental conditions of interest and potential differences in Rest baseline activity between children with ASD and TD children.

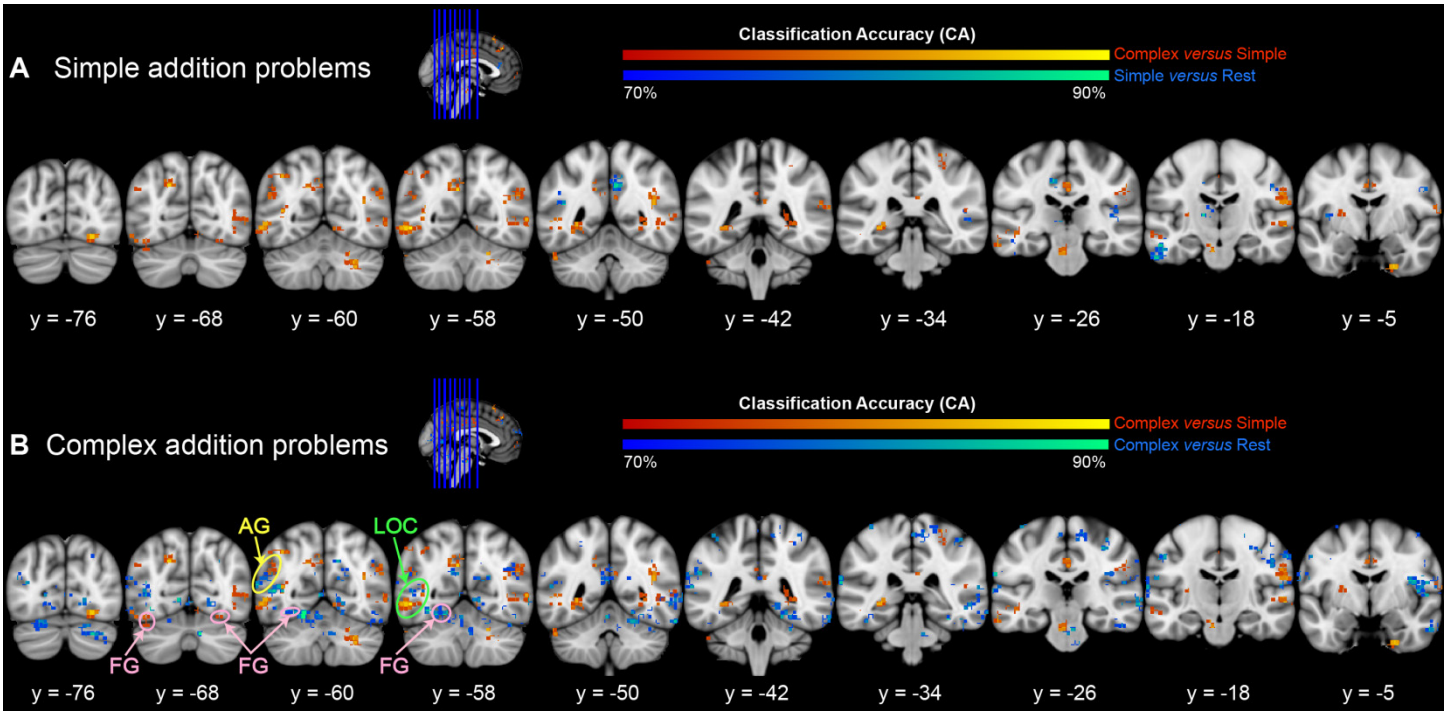

Figure S1. Multivariate brain activity classification maps distinguishing children with autism spectrum disorder (ASD) from typically developing (TD) children during arithmetic problem solving. (A) Comparison of between-group classification maps for Complex versus Simple addition problems (shown in red-yellow) and for Simple addition problems versus Rest (shown in blue-green). No brain regions showed overlapping effects in this case. **(B)** Comparison of between-group classification maps for Complex versus Simple addition problems (red-yellow) and for Complex addition problems versus Rest (blue-green). In both cases, significant effects were observed in ventral temporal-occipital cortex (VTOC) encompassing the fusiform gyrus (FG) and the inferior lateral occipital cortex (LOC), and in posterior parietal cortex encompassing the angular gyrus (AG). Multi-slices were created on the coronal axis and slices were equally spaced between each other (8 slices apart), except where additional slices were needed for comparison with results presented in **Figure 2**.

Table S1. Additional ASD Participant Information. Medication status for each of the 18 ASD participants.

Participant	Medication Status
ASD 1	
ASD 2	Claritin, Benadryl for seasonal allergies
ASD 3	
ASD 4	Zyrtec, Claritin for seasonal allergies
ASD 5	
ASD 6	
ASD 7	Zithromax 10 mg/Lexapro 5 mg
ASD 8	
ASD 9	Citalopram for social anxiety/shyness
ASD 10	Prozac/Risperidone
ASD 11	
ASD 12	
ASD 13	
ASD 14	
ASD 15	
ASD 16	Zyrtec, Rhinocort, Singulair, Digestive Enzymes, Priobiotics
ASD 17	Sertraline, Risperidone
ASD 18	Aripiprazole for irritability

ASD, autism spectrum disorder.

Table S2. Movement parameters (in mm) for autism spectrum disorder (ASD) and typically developing (TD) groups. Movement parameters did not differ between the two groups (all $p > .05$).

	ASD (n = 18)	TD (n = 18)	t-test	p-value
Maximum displacement	2.68, SD = 1.49	2.81, SD = 1.96	-0.22	.83
Maximum scan-to-scan displacement	2.05, SD = 1.39	1.95, SD = 1.41	0.23	.82
Mean scan-to-scan displacement	0.18, SD = 0.11	0.19, SD = 0.10	-0.35	.73
% Volumes repaired	1.59, SD = 1.77	1.84, SD = 1.97	-0.39	.69

df = (1, 34) for all analyses.

Table S3. Neuropsychological measures in autism spectrum disorder (ASD) and typically developing (TD) groups. Mean scores are shown for the ASD and TD groups on the two subtests of the Wechsler Individual Achievement Test – Second Edition (WIAT-II) scale and on the four working memory measures of the Working Memory Test Battery for Children (WMTB-C).

Measure	**ASD (*n* = 18)**	**TD (*n* = 18)**	***t*-test**	***p*-value**
WIAT-II Math				
Numerical Operations	119.61, SD = 20.94	103.94, SD = 14.00	2.638	.012*
Math Reasoning	111.22, SD = 11.14	104.78, SD = 11.53	1.520	.138
WMTB-C				
Counting Recall	94.53, SD = 19.58	91.44, SD = 13.42	0.546	.589
Backwards Digit Recall	102.47, SD = 19.53	97.11, SD = 20.55	0.790	.435
Digit Recall	114.00, SD = 22.15	106.75, SD = 14.10	1.122	.270
Block Recall	88.89, SD = 18.38	93.89, SD = 13.89	-0.921	.364

df = (1, 34) for all analyses.
*$p < .05$.

Supplemental References

1. Cox RW (1996): AFNI: software for analysis and visualization of functional magnetic resonance neuroimages. *Comput Biomed Res* 29:162-173.
2. Nichols T, Hayasaka S (2003): Controlling the familywise error rate in functional neuroimaging: a comparative review. *Stat Methods Med Res* 12:419-446.
3. Muller KR, Mika S, Ratsch G, Tsuda K, Schölkopf B (2001): An introduction to kernel-based learning algorithms. *IEEE Transactions on Neural Networks* 12:181–201.
4. Haynes JD, Sakai K, Rees G, Gilbert S, Frith C, Passingham RE (2007): Reading hidden intentions in the human brain. *Curr Biol* 17:323–328.
5. Abrams DA, Ryali S, Chen T, Balaban E, Levetin D J, Menon V (2012): Multivariate activation and connectivity patterns discriminate speech intelligibility in Wernicke's, Broca's, and Geschwind's areas. *Cereb Cortex* doi:10.1093/cercor/bhs165.
6. Pereira F, Mitchell T, Botvinick M (2009): Machine learning classifiers and fMRI: a tutorial overview. *Neuroimage* 45:S199-S209.
7. Cho S, Ryali S, Geary DC, Menon V (2011): How does a child solve 7 + 8? Decoding brain activity patterns associated with counting and retrieval strategies. *Dev Sci* 14:989-1001.
8. Stark CEL, Squire LR (2001): When zero is not zero: The problem of ambiguous baseline conditions in fMRI. *Proc Natl Acad Sci U S A* 98:12760-12766.